Proceedings of the 9ICEG
9th International Congress on Environmental Geotechnics
25-28 June, 2023 | Chania, Greece

https://doi.org/10.53243/ICEG2023-170

Cone penetrometer based on time domain reflectometry and laser induced fluorescence for contaminated site investigation

Qi-meng Guo[1,2,3], Liang-tong Zhan[1,2,*], Shun-yu Wang[1,2], Yun-min Chen[1,2], Qing-yi Mu[4], and Zhen-yu Yin[3]

[1]*Institution of Geotechnical Engineering, Zhejiang University, Hangzhou, China*

[2]*MOE Key Laboratory of Soft Soils and Geoenvironmental Engineering, Zhejiang University, Hangzhou, China*

[3]*Department of Civil and Environmental Engineering, The Hong Kong Polytechnic University, Hong Kong, China*

[4]*Department of Civil Engineering, Xi'an Jiaotong University, Xi'an, China*

**Corresponding author: Liang-tong Zhan, E-mail: zhanlt@zju.edu.cn*

ABSTRACT

The rapid characterization of soil and groundwater contamination is always a focus of environmental geotechnics, which stimulates the development of some advanced site characterization tools. This paper developed a novel cone penetrometer to identify soil ionic contaminants, groundwater dissolved organic matters (DOMs), and polycyclic aromatic hydrocarbons (PAHs) based on laser-induced fluorescence (LIF) and time domain reflectometry (TDR). The characteristic excitation wavelengths (325 nm) for defining the presence and extent of groundwater DOMs were found using excitation-emission-matrix spectra. On the other hand, to increase the detection depth of previous TDR penetrometers, the TDR module configuration (non-conductor shaft diameter and core material) was improved based on a spatial weighting analysis of the electromagnetic field using a seepage analysis software. Then, an integrated cone penetrometer consisting of a LIF module (two downhole ultraviolet lights to induce fluorescence and one industrial endoscope behind a sapphire window to capture the underground images) and a TDR module (four semicircle-shaped conductors circled PEEK shaft) was developed. Finally, the proposed novel penetrometer innovatively realized in-situ detection of groundwater DOMs based on 325 nm laser-induced fluorescence. The soil ionic contaminants and PAHs could also be characterized by electrical conductivity from TDR waveforms and fluorescence intensity from 275nm laser inducing respectively. The tool, successfully applied to a 30m-depth contamination detection in Woqishan Landfill, could hammer complex scenarios like landfills and petrochemical contaminated sites.

Keywords: soil and groundwater contamination; dissolved organic matters; time domain reflectometry; laser-induced fluorescence; penetrometer; complex scenarios

1 INTRODUCTION

By 2020, there are more than 650 large-scale sanitary landfills (with liners), and more than 27,000 small- or medium-scale simple landfills (without liners) distributed in China, covering an area of 20,000 km^2 (equivalent to the land area of Slovenia) (Lee et al., 2020). In these landfills, 60 billion tons of solid wastes are being stored, of which municipal solid wastes (MSW), construction and demolition wastes (CDW), and industrial solid wastes (ISW) accounts for 13.8%, 34.5%, and 51.7% respectively (Guo et al., 2021; Guo et al., 2022). According to the investigation of China National Environmental Monitoring Centre (CNEMC, 2020), the groundwater and soil around 85% of the studied 345 simple landfills were contaminated, e.g., the chemical oxygen demand (COD) and ammonia nitrogen of water sampled from the depth of 30 m in a landfill in Beijing exceeded 10 mg/L and 1.50 mg/L respectively, which means about several square kilometres of the surrounding groundwater cannot be used by humans and livestock (An et al., 2013). Especially, due to the variety of solid wastes stored in landfills, the groundwater and soils are usually polluted by multiple contaminants including inorganic matters (heavy metals, dissolved compounds, etc.), organic matters (dissolved organic matters, polycyclic aromatic hydrocarbons, etc.), and microorganisms (Siddiqua et al., 2022; Iravanian et al., 2020). Therefore, the development of advanced site characterization tools (ASCTs) for rapid identification of multiple

contaminants beneath the deep ground has become a technology focus for geo-environmental engineers caring about the subsurface environment in landfills.

Some popular ASCTs are commonly combined with cone penetration test (CPT) to measure the environmental parameters of interest through direct contact in environmental geotechnics (ITRC, 2019; Abdelhalim et al., 2021). Typical CPT based site contamination characterization tools have three main development directions, viz. membrane interface probe (MIP) for volatile organic compounds (VOCs) detection, laser-induced fluorescence (LIF) for polycyclic aromatic hydrocarbons (PAHs) detection, and time domain reflectometry (TDR) for electrical properties. MIP, proposed by Christy (1998), consists of a probe fitted with a small gas permeable membrane connected to flowing stream of inert carrier gas that is directed uphole to a photo ionisation detector (PID) or flame ionisation detector (FID). MIP is usually equipped with a block heater to vaporize VOCs underground (ASTM, D7352-17; Mousavi et al., 2021); There are two concerned ASCTs based on LIF, viz. optical image profiler (OIP) (McCall et al., 2018), and Ultra-Violet Optical Screening Tool (UVOST) (Dakota Technologies, 2018). Electrons in the PAHs molecules will jump to a high-energy state after being excited by UV light, but these electrons are unstable and active, which means they will return to some normal and lower-energy states with fluorescence release, that is the so-called LIF (Bujewski & Rutherford, 2000). The OIP equipped with 275 nm UV light and UVOST equipped with 350 nm UV light just evaluate soil contamination by analysing the LIF hue and intensity. However, no matter VOCs or PAHs, they are usually insoluble, which basically appear in industrial sites or fuel leakage scenarios; For MSW landfills, the organic contaminants are mainly dissolved (like humic acids and amino acids dissolved in leachate or groundwater), so how to expand the application boundary of ASCTs and realize the detection of dissolved organic matters (DOMs) has become a frontier and innovative research. On the other hand, TDR penetrometers were developed by scholars for electrical properties (dielectric constant and electrical conductivity) at various depths (Miyamoto et al., 2012; Zhan et al., 2021). The general practice of using a TDR penetrometer was to place conductors around a non-conductor shaft, which is usually polymer organic materials with low strength (Zhan et al., 2015). Therefore, once the detection depth exceeds 10 m, TDR penetrometers will often suffer from shear failure. How to improve the penetrometer strength and achieve deep ground detection of 20 – 30 m has become an issue to be solved.

This research aims to propose a CPT-based ASCT that can detect multiple contaminants including electrical properties, groundwater DOMs and soil PAHs. The equipment development includes two major difficulties: (1) how to assemble a LIF module that can detect DOMs; (2) How to enhance the strength of TDR module. The excitation-emission-matrix spectra (EEMS) helped to find the characteristic excitation wavelength of DOMs, viz. 325 nm UV light; Sensitivity analysis by GeoStudio helped to achieve TDR module configuration optimization leading to strength improvement strategy; Finally, a novel integrated cone penetrometer consists of TDR module (for detecting electrical properties) and LIF module (for detecting DOMs and PAHs) was developed. The ASCT was successfully applied in the investigation of Woqishan Landfill, China.

2 METHODOLOGY

Figure 1 shows the research & development methodology of this study. For identifying DOMs in landfill groundwater, the LIF module was used to evaluate their contents by exciting and analysing their fluorescence reaction. First, the characteristic excitation wavelength of landfill leachate was identified through EEMS test, and then the corresponding excitation optical element can be determined. Thus, an industrial endoscope was chosen as the fluorescence capture element to coordinate the excitation optical element leading to the assembling of LIF module.

For inorganic contaminants such as heavy metals and dissolved compounds which usually exist in the form of ionic compounds, the strength-enhanced TDR module (which can work in the depth of 20 – 30 m) was used to evaluate their contents by analysing electrical properties (dielectric constant and electrical conductivity) of soil or groundwater. First, the SEEP/W module in GeoStudio software was utilized to conduct sensitivity analysis of 4 potential cross section configurations of the TDR module. Based on the results of sensitivity analysis, the optimal configuration of TDR module was determined and a strength improvement strategy was proposed. Accordingly, a polyether ether ketone (PEEK) shaft, 4 probe-shape conductors, and a high-strength stainless steel rod were combined to manufacture the TDR module.

Finally, the LIF module and the TDR module were integrated to produce a novel cone penetrometer, which was applied to investigate the soil and groundwater environment around Woqishan Landfill, Wenzhou city, China. The investigation outcome validate the applicability of this equipment.

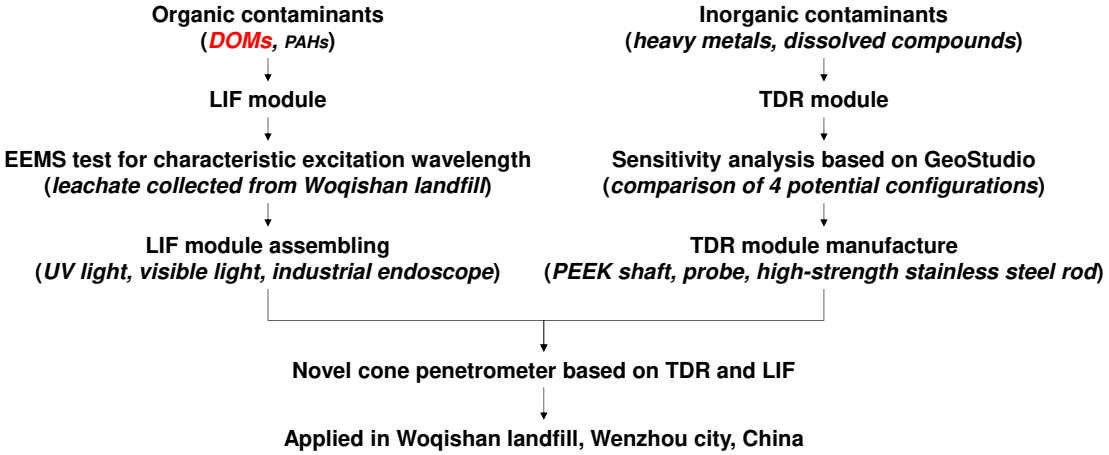

Figure 1. *Research & development methodology of cone penetrometer based on TDR and LIF*

3 RESEARCH AND DEVELOPMENT OF LIF MODULE

3.1 EEMS test for characteristic excitation wavelength of groundwater DOMs

When substances with fluorophores absorb excitation light, the electrons that obtain energy undergo a transition and, after energy transfer, the electrons release energy back to the ground state, emitting light in the form of fluorescence. EEMS is a 3D scan measured by a fluorescence spectrophotometer, resulting in a contour plot of excitation wavelength vs. emission length vs. fluorescence intensity (Yu et al., 2020). To determine the characteristic excitation wavelength of DOMs in landfills, the leachate from Woqishan Landfill, Wenzhou city and Tianziling landfill, Hangzhou city was sampled for EEMS test. For comparison, EEMS tests were also conducted for clean silt, clean water, soil-leachate mixture with a mass ratio of 9:1, soil-leachate mixture with a mass ratio of 8:2, soil-leachate mixture with a mass ratio of 7:3, and soil-leachate mixture with a mass ratio of 6:4. The testing equipment is FLS920 fluorescence spectrometer of Edinburgh Instruments. The used light source of FLS920 is Xe900 continuous xenon lamp, which can provide a steady-state spectral range of 200 – 2600 nm. The detector is single photon counting PMT. According to current studies (Li et al., 2023), the wavelength range of the excitation UV light was set from 270 nm to 350 nm, and the wavelength step was 5 nm. The corresponding emission spectrum was recorded to plot the EEMS.

Figure 2 shows the test results of fluorescence spectrometer. The ordinate represents the excitation light wavelength range, and the abscissa represents the emission light wavelength range. By comparing Figure 2a and Figure 2b, it was found that the leachate would produce the most intense fluorescence (the fluorescence intensity reached 9,000) under the excitation of 325 nm UV light, while the clean water had no significant fluorescence reaction. In particular, the fluorescence emission spectra of 7 mediums under 325 nm UV light excitation are shown in Figure 2c. It was found that the leachate has the most intense fluorescence of the wavelength greater than 380 nm (belonging to visible light), and clean soil and clean water have no fluorescence reaction; For the soil-leachate mixture, when the leachate content is low (the soil is unsaturated), the mixture has no fluorescence reaction. As the soil-leachate mass ratio decreases to approximate saturation of soil, the fluorescence intensity will suddenly increase. Especially, when the soil-leachate mass ratio exceeds 6:4 (supersaturated state), the fluorescence becomes significant. This supersaturated mixture should be better to be regarded as a kind of suspension (classified as aqueous medium). Figure 2d shows an EEMS test result of leachate from Huo et al. (2008), there are four typical fluorescence areas: (1) (Ex > 280 nm, Em > 380 nm) is connected with humic-like products; (2) (Ex < 280 nm, Em > 380 nm) is connected with fulvic-like lignin and other degraded plant; (3) (Ex > 250 nm, Em < 380 nm) is connected with tryptophan-like soluble microbial products; (4) (Ex < 250 nm, Em < 380 nm) is connected with tryptophan-like aromatic amino acid and amino-acid residue (Liu et al., 2015). Peak E in Figure 2d (the excitation wavelength and the emission wavelength is also near 325 nm and 420 nm respectively) was attributed to aromatic and aliphatic groups in the DOM fraction and commonly labelled as humic-like and fulvic-like, and related to the carbonyl and carboxyl in the humus. Obviously, the fluorescence phenomenon in this study is similar to that of Huo et al. (2008), so 325 nm can be determined as the characteristic light that can excite the fluorescence reaction of humic-like and fulvic-like DOM fraction in aqueous medium (Oloibiri et al.,

2017). Specially, the DOM can account for 80% of total organic carbon (TOC) concentration, ranging from 800 to 20,000 mg/L (Table 1) (Huo et al., 2008).

Table 1. *Composition of landfill leachate (Kjeldsen et al., 2002)*

Parameter	pH (no unit)	EC ($mS \cdot m^{-1}$)	TOC ($mg \cdot L^{-1}$)	BOD_5 ($mg \cdot L^{-1}$)	COD ($mg \cdot L^{-1}$)	Organic nitrogen ($mg \cdot L^{-1}$)
Range	4.5-9	250-3500	30-29000	20-57000	140-152000	14-2500

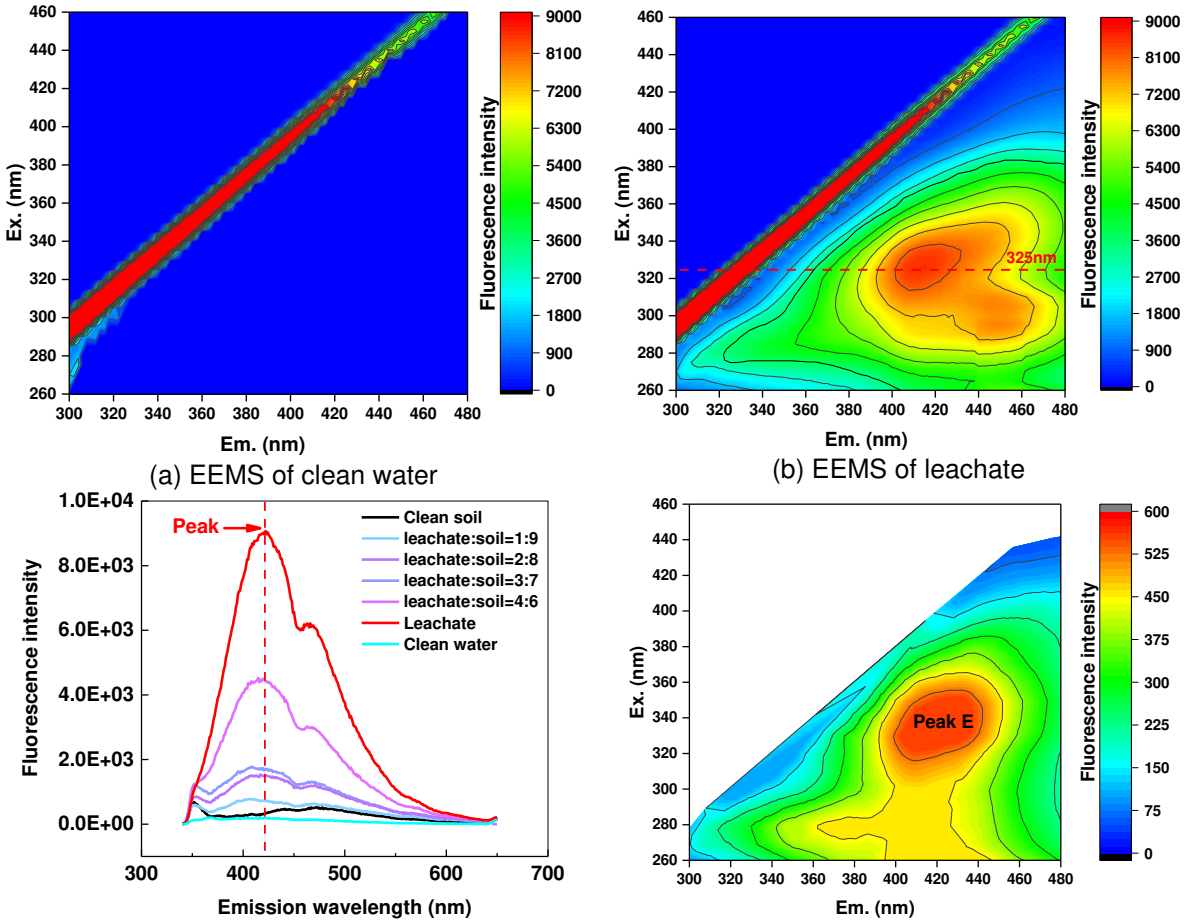

(a) EEMS of clean water (b) EEMS of leachate

(c) Fluorescence intensity with 325 nm excitation (d) EEMS of leachate from Huo et al. (2008)

Figure 2. *EEMS test results of leachate and the characteristic UV wavelength*

3.2 LIF module assembling

To assemble the LIF module, light sources and fluorescence capture advice should be carefully selected. The 325 nm UV light determined in Section 3.1 was chosen as the excitation source of DOM, and the 275 nm UV light was chosen as the excitation source of PAHs referring to McCall et al. (2018); At the same time, it is necessary to select a mini fluorescence capture advice which is suitable to be installed in a cone penetrometer and can realize a near-focus imaging subsurface; In addition, the internal components of the LIF module must be physically isolated from the external detected medium. The isolating component has to be required to be light transparent to ensure the stable fluorescence reaction. Meanwhile, since the equipment needs to be used in deep ground, the isolating component should be hard and have a good wear-resistance capability to avoid the abrasion of sands and gravels during the penetration. Based on the above principals, the LIF module was assembled as shown in Figure 3.

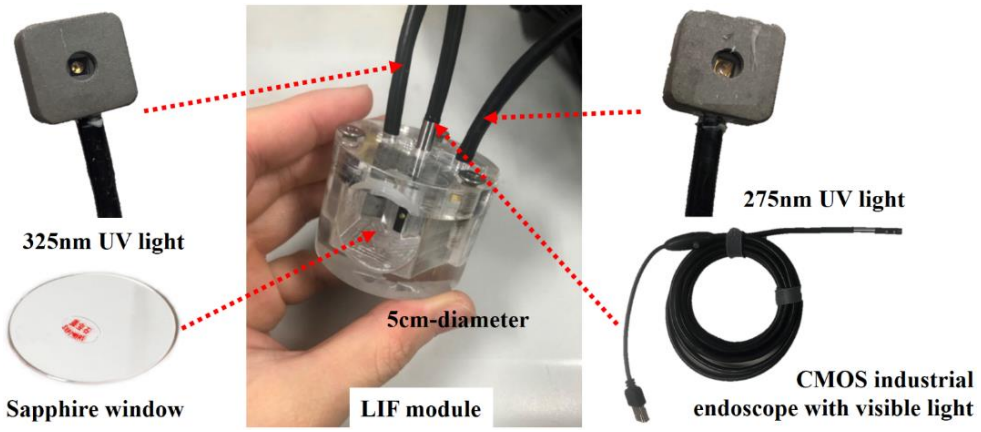

Figure 3. *Configuration of the LIF module*

Figure 3 shows the configuration of the LIF module. The dimension of the UV lights is 20×20×10 mm. The fluorescence capture advice is a CMOS industrial endoscope with visible light. The length and width of the endoscope is 20mm and 4.9 mm respectively. It can capture objects in a 2–5 cm near-focus range. The visible LED guarantees the identification of the type of the detected mediums in a deep ground environment. The acquisition of the original image of detected mediums under visible light can help evaluate the contamination degree subsurface. Sapphire window with the Moh's hardness of 9 was chosen as the isolating component. Finally, the diameter of the whole LIF module was only 5 cm, which is easy to install into a cone penetrometer.

4 RESEARCH AND DEVELOPMENT OF TDR MODULE

4.1 Principles for sensitivity analysis based on GeoStudio

To improve the strength of the TDR module, it is necessary to determine the optimal configuration of the TDR module. Based on Zhan et al. (2015), sensitivity analysis of TDR module configuration can be conducted by using the SEEP/W module in GeoStudio software. A spatial weighting factor (w(x,y)) at each point for the spatial sensitivity of TDR probes can be expressed as follows:

$$w(x,y) = \nabla\Phi^2(x,y)/\iint \nabla\Phi_{eq}^2(x,y)\,dxdy \quad (1)$$

where $\Phi(x,y)$ is the electrical potential in the heterogeneous field; and $\Phi_{eq}(x,y)$ is the electrical potential in the equalized homogeneous field. $\Phi(x,y)$ and $\Phi_{eq}(x,y)$ could be computed using the SEEP/W module in the Geostudio software package.

The effective apparent dielectric permittivity of the penetrometer ($\varepsilon_{a,eff}$) is a weighted average of the apparent dielectric permittivity of the targeted medium ($\varepsilon_{a,t}$) and the apparent dielectric permittivity of the non-conductor shaft ($\varepsilon_{a,o}$) as follows:

$$\varepsilon_{a,eff} = \varepsilon_{a,o}\iint w_o(x,y)\,dxdy + \varepsilon_{a,t}\iint w_t(x,y)\,dxdy \quad (2)$$

$$\iint w_o(x,y)\,dxdy + \iint w_t(x,y)\,dxdy = 1 \quad (3)$$

where $w_o(x,y)$ and $w_t(x,y)$ are the weighting factors that are distributed in the shaft zone and the targeted medium zone respectively.

Based on the weighting factors, parameter *f* was defined as an influence area with a percent form:

$$f = 100\sum_{w_{hi}}^{w} w_i\,A_i/\iint w_i\,dA \quad (4)$$

where w_i is the weighting factor in a finite element mesh, w_{hi} is the maximum of all weighting factors, and A_i is the area of the finite element mesh.

4.2 Results of sensitivity analysis for 4 potential configurations

According to relevant experience (Redman & Deryck, 1994; Miyamoto et al., 2012; Zhan et al., 2015), sensitivity analysis was conducted on 4 potential configurations of four-probe TDR penetrometer. The sketch of TDR module is shown in Figure 4a. M1 is non-conductor shaft, M2 are 4 probes, and M3 is the targeted medium. S1 to S5 are boundary conditions. The electrical potential of S1 and S3 was set as 1, while the electrical potential of S2 and S4 was set as -1. The boundary condition of S5 was set as $\partial\Phi/\partial n = 0$, which means there will be no inflow or outflow of electrical energy on the boundary. Then the electrical potential around penetrometer can be obtained as Figure 4b. The potential contours around the penetrometer are symmetrically distributed. The potential around positive electrode increases to 1.0 from outside to inside, and the potential around negative electrode decreases to - 1.0 from outside to inside.

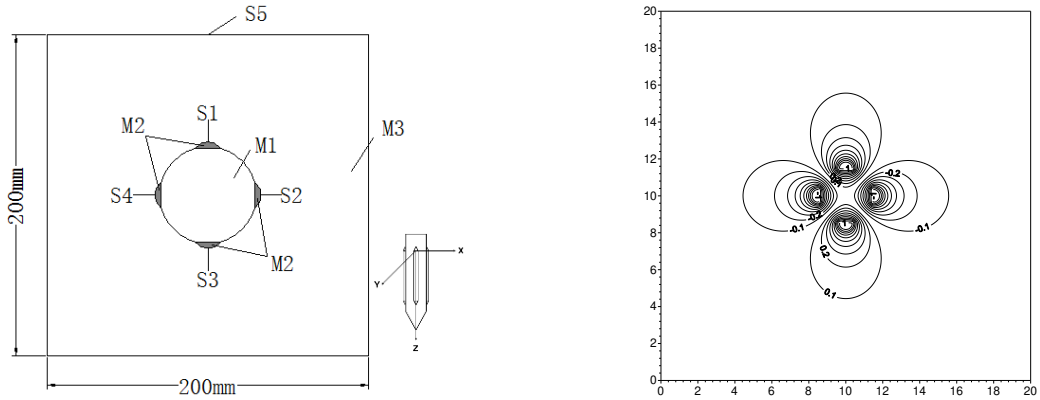

(a) Sketch of TDR module (b) Electrical potential around penetrometer

Figure 4. *Sketch of TDR module for sensitivity analysis and electrical potential analysis result*

The 4 potential configurations of the TDR module are as follows: (1) The 30mm-diameter (D) non-conductor shaft with four 8mm-diameter probes attached; (2) The 36mm-diameter (D) non-conductor shaft with four 8mm-diameter probes attached; (3) The 42mm-diameter (D) non-conductor shaft with four 8mm-diameter probes attached; (4) The 48mm-diameter (D) non-conductor shaft with four 8mm-diameter probes attached. The parameter f of 4 configurations is shown in Figure 5. Obviously, $f = 100\%$ in the whole area. The weighting factor (w_i) in the whole area was arranged from large to small, and the w_iA_i was accumulated from the largest (w_{hi}). When the $f = 50\%$, all accumulated meshes were painted as red, which means these red areas contribute 50% influence to the test results of TDR; When the $f = 90\%$, all accumulated meshes (excluding red areas) were painted as yellow, which means these yellow areas plus red areas contribute 90% influence to the test results of TDR.

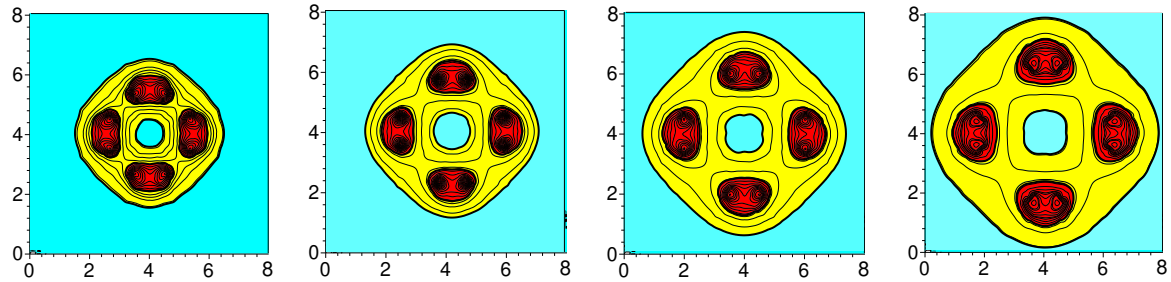

Figure 5. *Results of sensitivity analysis for 4 potential TDR module configurations*

It can be found from Figure 5 that the central part of the penetrometer cross section contribute little to the TDR test results (low-sensitivity area), where some high-strength materials can be filled to improve the whole strength of the TDR module. To note, if the diameter of the penetrometer is too small, the content of high-strength materials will be too few to strengthen the TDR module; If the diameter of the penetrometer is too large, the equipment will become non-portable. Therefore, the 42mm-diameter non-conductor shaft with four 8mm-diameter probes attached should be the optimal configuration.

4.3 TDR module manufacture

Based on Section 4.2, it was determined that the TDR module (Figure 6) consists of four semi-circularly shaped stainless steel probes, which are placed around a PEEK shaft (diameter: 42 mm) through steel

nails. The semi-circularly shaped stainless-steel conductor has a diameter of 8 mm and a length of 150 mm. One pair of two opposite stainless-steel conductor is connected to the inner conductor of the coaxial cable (impedance: 50 Ω) through soldering. The shield of the coaxial cable is connected to the other pair of opposite stainless-steel conductors. A high-strength steel rod (Tensile strength is 630 MPa and compressive strength is 500 MPa) was installed into the low-sensitivity area.

5 CONE PENETROMETER AND APPLICATION

5.1 Structure of the cone penetrometer based on LIF and TDR

Based on the LIF module in Section 3 and the TDR module in Section 4, the cone penetrometer based on LIF and TDR was assembled as shown in Figure 6. The length of the sensor fraction of the penetrometer is less than 30 cm, and the maximum diameter is 6 cm.

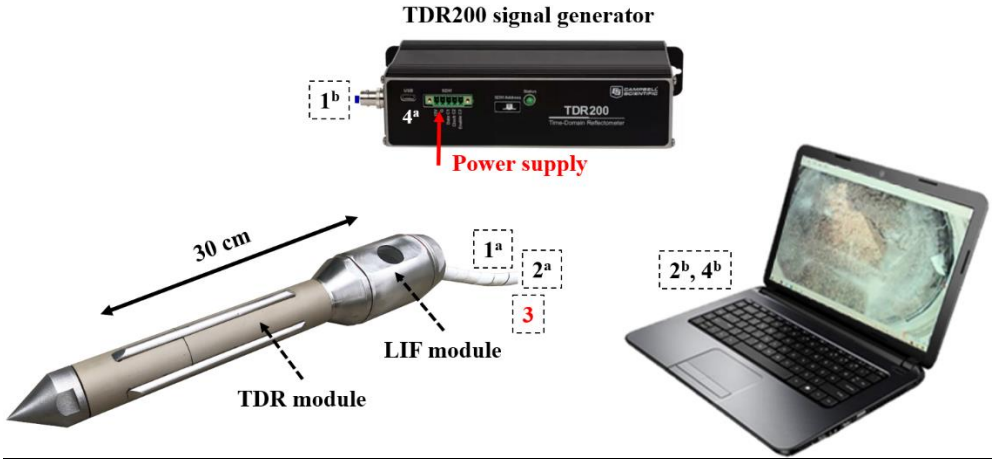

Figure 6. *Configuration of the detection system based on the penetrometer*

The whole detection system (Figure 6) consists of the penetrometer, TDR200 (provided by Campbell Scientific Inc.), and a laptop. The penetrometer has three interfaces (named as 1^a, 2^a, and 3). The 1^a interface should be connected with 1^b of TDR200 signal generator by coaxial cable leading to the transmission of electromagnetic wave. The 4^a of TDR200 should be connected with the laptop by a USB line for control and data communication. The 2^a of penetrometer can be connected with the laptop by a USB line directly for underground image analysis. The 3 is for power supply of UV lights.

In an investigation procedure for landfills, the penetrometer was penetrated into the ground. After one time of 30cm-penetration, a detection should be implemented. First, the detected medium should be observed through the sapphire window under the visible LED. If the detected medium is groundwater, the 325 nm UV light should be turned on to excite the fluorescence reaction of DOMs. The endoscope will capture the fluorescence image and deliver it to the laptop for DOMs analysis. Then the 325 nm UV light should be turned off, and the TDR200 should be started to obtain the TDR waveform for calculating electrical conductivity and dielectric constant of water; If the detected medium is soil, the light to be turned on should be the 275 nm UV light (for PAHs analysis), and the TDR waveform will be the characteristics of soils.

5.2 Application in Woqishan Landfill

Woqishan Landfill is located in Wenzhou city, China (Figure 7). It covers approximately 4.32 ha area and has a maximum filling height of 35.2 m. The volume of filled MSW is about 760,000 m^3. The landfill served from 1981 to 2002. To verify the feasibility of penetrometer, cone penetration test was implemented at three points (Figure 7) inside the landfill from December 17, 2020 to December 25, 2020.

Before on-site implementation, the penetrometer should be calibrated: (1) For the LIF module, first of all, five leachate specimens with a gradient concentration of DOM were prepared, and then fluorescence images of specimens were taken using the penetrometer. The images' mode was converted from RGB mode to HSV mode. The average of pixel values in the Value Channel of the image ($V_{average}$) should be calculated. Meanwhile, the COD content of specimens should be tested with a COD tester, and the COD value should be multiplied by 0.8 to obtain an estimated value of DOM. Finally, an

empirical formula for fluorescence intensity and DOM value can be calibrated for five specimens; (2) For TDR modules, considering the existence of PEEK shaft, the dielectric permittivity and electrical conductivity measured by TDR module need to be converted into that of soil around the probe through calibration. Mixtures of Ethanol (dielectric permittivity is about 16)–deionized water (dielectric permittivity is about 80) with different concentrations (from 0 to 100%, 20% by interval) were selected as target mediums to calibrate the dielectric permittivity. The dielectric permittivity of target medium measured by three-rod TDR probe and the TDR waveform obtained by TDR module were fitted to construct the dielectric permittivity calculation formula; NaCl solution with different concentrations (from 0 to 0.030 mol/L, 0.005 mol/L by interval) was used as target mediums to calibrate the electrical conductivity. The electrical conductivity of target medium measured by three-rod TDR probe and the TDR waveform measured by TDR penetrometer can be fitted to construct the electrical conductivity calculation formula.

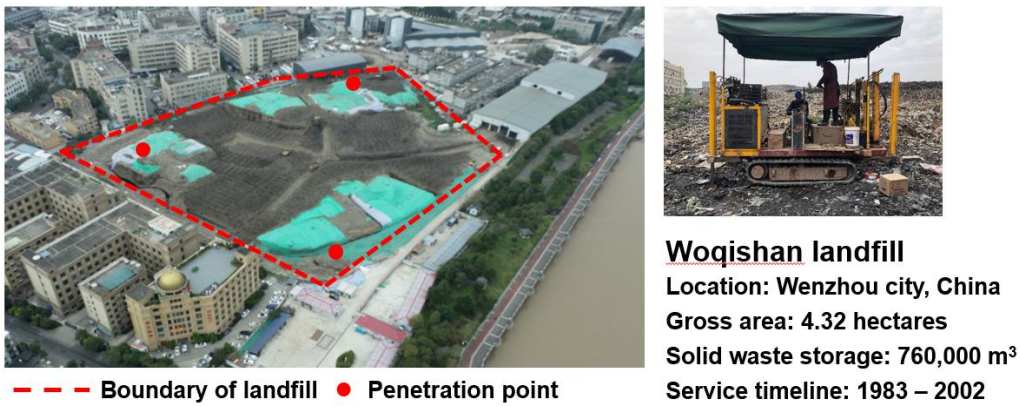

Figure 7. *Woqishan Landfill and application procedure*

Figure 8 shows one of the detection results during this application. In Figure 8a, 1-1, 2-1, and 2-2 are three adjacent soil EC profiles at the same penetration location. First of all, it was found that the strength-enhanced penetrometer realized a deep ground detection beyond a depth of 20 m, and the detection results of 1-1, 2-1, and 2-2 are well matched. It is worth noting that the EC at the waste layer exceeds 900 mS/m, while the EC at the clay layer drops to below 150 mS/m greatly, and characteristic fluorescence reactions were also found at the waste layer. Figure 8b shows the dynamic change of fluorescence reactions of an aqueous medium at the waste layer under the excitation of 325 nm UV light (Figure 8b-1 to Figure 8b-4 occurred in chronological order at the same groundwater contamination location). At first, the leachate occupied the entire pore space (Figure 8b-1), then the leachate gradually infiltrated into the waste body (Figure 8b-2, Figure 8b-3), and finally the waste body appeared inside the view where fluorescence almost faded (Figure 8b-4). To better illustrate the applicability of the penetrometer, five test results of the penetrometer and sampling tests were compared in Figure 8c. It can be found the test results of COD by the penetrometer (based on the 325 nm fluorescence reaction) are smaller than that of the sampling test, because DOMs are only parts of the contaminants related to COD (e.g., some micro-organisms cannot be assessed in this situation). The average relative error is 34.8%, and it can be found that the higher the true value of COD, the smaller the relative error. To sum up, the effectiveness of the penetrometer for contaminated site semi-quantitative investigation could be validated.

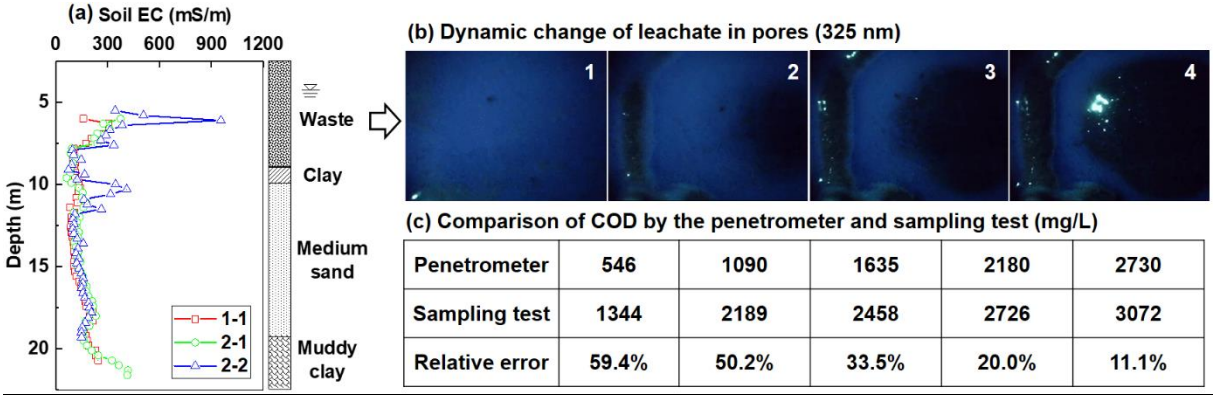

(c) Comparison of COD by the penetrometer and sampling test (mg/L)

Penetrometer	546	1090	1635	2180	2730
Sampling test	1344	2189	2458	2726	3072
Relative error	59.4%	50.2%	33.5%	20.0%	11.1%

Figure 8. *Application results of the penetrometer*

6 CONCLUSIONS

Aiming at the problems that existing LIF-based ASCTs cannot realize the rapid detection of DOMs, which are common in landfills, and existing TDR-based cone penetrometers cannot realize a deep ground detection (20-30 m) due to the low strength of non-conductor shaft, this study solved the above issues through EEMS tests and sensitivity analysis by GeoStudio software. Accordingly, a novel cone penetrometer based on laser induced fluorescence and time domain reflectometry was developed. The applicability of this equipment was validated by a contaminated site investigation. Details are as follows:

(1) The characteristic excitation wavelength of landfill leachate is 325 nm UV light, and the fluorescence reaction comes from humic-like and fulvic-like DOMs in aqueous medium; The LIF module composed of 325nm UV light, 275nm UV light, industrial endoscope, and sapphire window can be assembled to realize the detection of underground DOMs and PAHs.

(2) The probes of the four-probe TDR module is surrounded by a high-sensitivity area (f = 50%). The non-conductor shaft and targeted medium occupy a medium-sensitivity area (f = 90%). There is a low-sensitivity area in the centre of the shaft, where high-strength materials can be filled to improve the overall strength of the TDR module; a TDR module consisting of four semi-circularly shaped stainless steel probes, which are placed around a PEEK shaft through steel nails, was assembled.

(3) A novel cone penetrometer based on LIF module and TDR module was developed. Accordingly, a detection system including the penetrometer, TDR200 and laptop was also proposed. This system can realize the rapid detection of underground electrical properties, DOMs and PAHs in-situ, and was successfully applied to contamination investigation of Woqishan Landfill.

7 ACKNOWLEDGEMENTS

This work was supported by National Key Research and Development Program of China (2018YFC1802300), Academic Star Training Program for Ph.D. Students of Zhejiang University (No.2022045), and Key Research and Development Program of Zhejiang Province (2019C03107).

REFERENCES

Abdelhalim, R. A., Ramli, H., & Selamat, M. R. (2021). Cone penetration measurements in oil-contaminated sand stabilized by lateritic soil and potential usage in concrete mix. Case Studies in Construction Materials. 15(Dec), e00580.

An, D., Jiang, Y., Xi, B., Ma, Z., Yang, Y., Yang, Q., Li, M., & Zhang, J. (2013). Analysis for remedial alternatives of unregulated municipal solid waste landfills leachate-contaminated groundwater. Frontiers of Earth Science, 7, 210-319.

ASTM D7352-17. (2017). In Standard Practice for Direct Push Technology for Volatile Contaminant Logging with the Membrane Interface Probe (MIP). ASTM International, 100 Barr Harbor Dr., West Conshohocken, PA. www.astm.org.

Bujewski, G., & Rutherford, B. (1995). Innovative Technology Verification Report: The Site Characterization and Analysis Penetrometer System (SCAPS) Laser-Induced Fluorescence (LIF) Sensor and Support System. https://archive.epa.gov/nrmrl/archive-etv/web/pdf/01_vr_usn_penetrometer.pdf

China National Environmental Monitoring Centre. (2020). China Ecological Environment Statistical Annual Report in 2020. (in Chinese) http://www.cnemc.cn/jcbg/zghjtjnb/202212/P020221207619939813426.pdf

Christy, T. M. (1998). A permeable membrane sensor for the detection of violate compounds in soil. https://clu-in.org/download/contaminantfocus/dnapl/detection_and_site_characterization/mippapertmc_geoprobe.pdf

Dakota Technologies. Introduction of UVOST. https://www.dakotatechnologies.com/services/uvost

Guo, W., Xi, B., Huang, C., Li, J., Tang, Z., Li, W., Ma, C., & Wu, W. (2021). Solid waste management in China: Policy and driving factors in 2004–2019. Resources, Conservation & Recycling, 173, 105727.

Guo, Q. M., Zhan, L. T., Shen, Y. Y., Wu, L. B., & Chen, Y. M. (2022). Classification and quantification of excavated soil and construction sludge: A case study in Wenzhou, China. Frontiers of Structural and Civil Engineering, 16, 202–213.

Huo, S. L., Xi, B. D., Yu, H. C., Fan, S. L., Jing, S., & Liu, H. L. (2008). A laboratory simulation of in situ leachate treatment in semi-aerobic bioreactor landfill. Water S. A., 34(1), 133-140.

Iravanian, A. & Ravari, S. O. (2020). Types of Contamination in Landfills and Effects on The Environment: A Review Study. Earth and Environmental Science, 614, 012083.

Kjeldsen, P., Barlaz, M. A., Rooker, A. P., Baun, A., Ledin, A., & Christensen, T. H. (2002). Present and long term composition of MSW landfill leachate – a review. Critical Reviews in Environmental Science and Technology, 32, 297-336.

Lee, R. P., Meyer, B., Huang, Q., & Voss, R. (2020). Sustainable waste management for zero waste cities in China: potential, challenges and opportunities. Clean Energy, 4(3), 169-201.

Li, W., Li, X., Han, C., Gao, L., Wu, H., & Li, M. (2023). A new view into three-dimensional excitation-emission matrix fluorescence spectroscopy for dissolved organic matter. Science of The Total Environment, 855(Jan), 158963.

Liu, Z. P., Wu, W. H., Shi, P., Guo, J. S., & Cheng, J. (2015). Characterization of dissolved organic matter in landfill leachate during the combined treatment process of air stripping, Fenton, SBR and coagulation. Waste Management, 41(Jul), 111-118.

McCall, W., Christy, T.M., Pipp, D.A., Jaster, B., White, J., Goodrich, J., Fontana, J., & Doxtader, S. (2018). Evaluation and application of the optical image profiler (OIP) a direct push probe for photo-logging UV-induced fluorescence of petroleum hydrocarbons. Environtal Earth Sciences, 77, 374.

Miyamoto, Y., K. Fukami, & J. Chikushi (2012), Simultaneous measurement of soil water and soil hardness using a modified time domain reflectometry probe and a conventional cone penetrometer, Soil Use Manage., 28(2), 240– 248.

Mousavi, M. S., Feng, Y., McCann, J., & Eun, J. (2021). In Situ Characterization of Municipal Solid Waste Using Membrane Interface Probe (MIP) and Hydraulic Profiling Tool (HPT) in an Active and Closed Landfill. Infrastructures, 6, 33.

Oloibiri, V., Coninck, S. D., Chys, M., Demeestere, K., Hulle, S. W. H. V. (2017). Characterisation of landfill leachate by EEM-PARAFAC-SOM during physical-chemical treatment by coagulation-flocculation, activated carbon adsorption and ion exchange. Chemoshere, 186, 873-883.

Redman, J. D., & S. M. Deryck. (1994). Monitoring nonaqueous phase liquids in the subsurface with multilevel time domain reflectometry probes, paper presented at Symposium and Workshop on Time Domain Reflectometry in Environmental, Infrastructure and Mining Application, U.S. Bur. of Mines, Sept 7– 9, Evanston, Ill.

Siddiqua, A., Hahladakis, J. N. & Al-Attiya, W. A. K. A. (2022). An overview of the environmental pollution and health effects associated with waste landfilling and open dumping. Environmental Science and Pollution Research, 29, 58514–58536.

The Interstate Technology & Regulatory Council (ITRC). (2019). Implementing Advanced Site Characterization Tools. https://asct-1.itrcweb.org/

Yu, J., Xiao, K., Xue, W., Shen, Y. X., Tan, J., Liang, S., Wang, Y., Huang, X. (2020). Excitation-emission matrix (EEM) fluorescence spectroscopy for characterization of organic matter in membrane bioreactors: Principles, methods and applications. Frontiers of Environmental Science & Engineering, 14(2), 31.

Zhan, L. T., Mu, Q. Y., Chen, Y. M., & Ke, H. (2015). Evaluation of measurement sensitivity and design improvement for time domain reflectometry penetrometers. Water Resources Research, 51(4), 2994-3006.

Zhan, L. T., Guo, Q. M., Mu, Q. Y., & Chen, Y. M. (2021). Detection of ionic contaminants in unsaturated soils using time domain reflectometry penetrometer. Environmental Earth Sciences, 80, 330.